Molecular Psychiatry (2017) 00, 1–9

www.nature.com/mp

ORIGINAL ARTICLE

The dynamics of stress: a longitudinal MRI study of rat brain structure and connectome

R Magalhães[1,2], DA Barrière[3], A Novais[1,2], F Marques[1,2], P Marques[1,2], J Cerqueira[1,2], JC Sousa[1,2], A Cachia[3,4,5,6], F Boumezbeur[7], M Bottlaender[7], TM Jay[3,4,8], S Mériaux[7] and N Sousa[1,2]

Stress is a well-established trigger for a number of neuropsychiatric disorders, as it alters both structure and function of several brain regions and its networks. Herein, we conduct a longitudinal neuroimaging study to assess how a chronic unpredictable stress protocol impacts the structure of the rat brain and its functional connectome in both high and low responders to stress. Our results reveal the changes that stress triggers in the brain, with structural atrophy affecting key regions such as the prelimbic, cingulate, insular and retrosplenial, somatosensory, motor, auditory and perirhinal/entorhinal cortices, the hippocampus, the dorsomedial striatum, nucleus accumbens, the septum, the bed nucleus of the stria terminalis, the thalamus and several brain stem nuclei. These structural changes are associated with increasing functional connectivity within a network composed by these regions. Moreover, using a clustering based on endocrine and behavioural outcomes, animals were classified as high and low responders to stress. We reveal that susceptible animals (high responders) develop local atrophy of the ventral tegmental area and an increase in functional connectivity between this area and the thalamus, further spreading to other areas that link the cognitive system with the fight-or-flight system. Through a longitudinal approach we were able to establish two distinct patterns, with functional changes occurring during the exposure to stress, but with an inflection point after the first week of stress when more prominent changes were seen. Finally, our study revealed differences in functional connectivity in a brainstem–limbic network that distinguishes resistant and susceptible responders before any exposure to stress, providing the first potential imaging-based predictive biomarkers of an individual's resilience/vulnerability to stressful conditions.

Molecular Psychiatry advance online publication, 5 December 2017; doi:10.1038/mp.2017.244

INTRODUCTION

Stress is an essential component of life, as every living organism has to continuously face challenges. However, there is a remarkable repertoire and heterogeneity in the way each individual responds to stressful conditions.[1–3] These contrasting patterns of responses reveal whether the stress exposure triggered a positive adaptation or a detrimental maladaptive process.[4] Whereas the first will be critical to re-establish homeostasis, the latter is known to trigger deleterious effects across different parts of the organism, including the central nervous system. These deleterious effects may help explain the development of psychopathologies such as major depression, anxiety and posttraumatic stress disorders.[2,5–8] Finally, the role of various factors such as prenatal and early-life exposure to stress,[9–11] personality traits,[12–14] epigenetic mechanisms[13,15] and the microbiome[16–18] as modulators of the response to stress should not be neglected.

The impact of stress in the brain has been studied at different levels: from the molecular[19–21] to the cellular[22–24] to the network levels.[25–27] However, so far, mainly as a result of technical limitations, studies designed to assess the impact of stress upon the central nervous system have only provided a snapshot perspective of what happens in a particular moment in time and, thus, preclude the understanding of the dynamics of the shifts that occur in individuals exposed to prolonged stressful conditions. To the best of our knowledge, a single study has used resting-state functional magnetic resonance imaging (MRI) to characterize an animal model of chronic stress;[26] in this study an increased functional connectivity was found within somatosensory, visual and default mode networks in stressed animals. Two other studies have associated differentiated responses to stress (resilient or susceptible) with different changes in volume and fractal anisotropy in several brain regions using both mouse and rat models and *ex vivo* MRI.[28,29] Areas reported to be altered include modulators of the hypothalamic–pituitary–adrenal axis (hippocampus and bed nucleus of stria terminalis) and areas related to the development of depressive-like behaviour and fear management (raphe nuclei and periaqueductal grey matter (PAG)).

Revealing the mechanisms that underlie the development of vulnerability or resistance to stress is crucial for the development of new treatments for stress-related disorders of the brain.[2] On the other hand, identifying imaging markers that detect susceptibility to the adverse effects of stress would facilitate clinical practice and outcomes,[30] by allowing earlier interventions.

In the present study, we designed a longitudinal and multimodal approach to assess the dynamics of the changes triggered by stress exposure in the structure and in the resting-state

[1]Life and Health Sciences Research Institute (ICVS), School of Medicine, University of Minho, Braga, Portugal; [2]ICVS/3B's, PT Government Associate Laboratory, Braga/Guimarães, Portugal; [3]Physiopathologie des Maladies Psychiatriques, UMR_S 894 Inserm, Centre de Psychiatrie et Neurosciences, Paris, France; [4]Université Paris Descartes, Sorbonne Paris Cité, Paris, France; [5]Laboratoire de Psychologie du développement et de l'Education de l'Enfant, CNRS UMR, Paris, France; [6]Institut Universitaire de France, Paris, France; [7]Neurospin, JOLIOT, CEA, Gif/Yvette, France and [8]Faculté de Médecine Paris Descartes, Service Hospitalo-Universitaire, Centre Hospitalier Sainte-Anne, Paris, France. Correspondence: Dr N Sousa, School of Medicine, Life and Health Sciences Research Institute (ICVS), University of Minho, 4710-057 Braga, Portugal.
E-mail: njcsousa@med.uminho.pt
Received 10 May 2017; revised 4 August 2017; accepted 6 September 2017

functional connectome of the rat brain. Moreover, and having in mind the heterogeneity in the stress response of different individuals, we categorized animals exposed to stress in high and low responders based on a composite of behavioural and endocrine longitudinal assessment. Such approaches allowed us to determine: (1) the temporal dynamics of the impact of stress exposure on the structure and functional connectome of the rat brain; (2) the contrasting pattern of changes in networks and nodes between high- and low-stress responders; (3) the temporal dynamics of adaptive versus maladaptive shifts and (4) the pre-existing patterns of the neuromatrix (an aggregate of neurons that works as a self sustained system and as a dynamic network[31,32]) that would predict a differential response to stress exposure.

MATERIALS AND METHODS

Animal groups and experimental design

A total of 72 male Wistar rats with 8 weeks of age (Janvier, Le Genest-St-Isle, France) were housed in groups of two in standard laboratory conditions (lights on: 0700 to 1900 h; ± 22 °C of temperature; relative humidity of 55%) and had *ad libitum* access to food and water. Animals were divided into 2 sets: set one with 40 animals (25 stress+15 controls) was assessed after 21 days of stress; set two with 32 animals (24 stress+8 controls) was assessed at 3 time-points: before stress (day 0); after a week of exposure to stress (day 7); and after 3 weeks of exposure to stress (day 21). Because of the novelty of the methods applied no power analysis was possible to be conducted. The sample size was chosen by considering previous published work using rat MRI and previous stress characterization studies. Animals assigned to the stress group were exposed to a chronic unpredictable stress (CUS) protocol for a period of 3 weeks. Assessment included a measure of anxiety-like behaviour (time spent in the open arms of the elevated plus maze (EPM)), blood corticosterone levels and *in vivo* MRI at various intervals. All assessments were conducted on consecutive days in the order described. To avoid a possible impact of circadian rhythms, the order by which the animals were assessed was randomized along the days. For further information regarding the stress protocol, corticosterone quantification and behaviour, see Supplementary Information.

All experiments were performed in accordance with the recommendations of the European Union Directive (2010/63/EU) and the French legislation (Decree no. 87/848) for use and care of laboratory animals. The protocols have been approved by the Comité d'Éthique en Expérimentation Animale du Comissariat à l'Énergie Atomique et aux Énergie Alternatives–Direction des Sciences du Vivant Île de France (CETEA/CEA/DSV IdF) under protocol ID 12-058.

MRI acquisitions

MR examinations were done with a preclinal BioSpec 11.7T scanner (Bruker, Ettlingen, Germany) running on Paravision 6.0. A 72 mm diameter volume coil used for transmission and a 4-channel phased array surface coil for reception. The scanning protocol consisted in acquiring a resting-state functional MRI data set using a multi-shot spin-echo echo planar imaging sequence with the following parameters: interleaved acquisition with 3 segments, repetition time (TR) = 2000 ms, echo time (TE) = 17.5 ms, flip angle (FA) = 90°, 450 repetitions, acquisition matrix = $20 \times 64 \times 64$, slice thickness = 0.75 mm, inter slice gap = 0.2375 mm and in plane resolution of 0.375×0.375 mm^2, for a field of view (FoV) of $24 \times 24 \times 19.75$ mm^3. To reduce the possible effects of anaesthesia during resting-state functional MRI, the level of isoflurane was adjusted so as to maintain the breathing rate between 70 and 80 breaths per min. To reduce artefacts resulting from breathing movements, a trigger was used so that data were only acquired during the stable stages of the breathing wave. In addition, a T_2-weighted RARE (rapid imaging with relaxation enhancement) anatomical image was acquired with the following parameters: turbo-factor = 16, TR = 1500 ms, TE = 5.5 ms, 1 repetition, acquisition matrix = 192×192 with 48 sagittal slices, slice thickness = 0.3 mm, in-plane resolution of 0.15×0.15 mm^2 and a FoV of $28.8 \times 14.4 \times 28.8$ mm^2 covering the entire brain. All the data were reconstructed using in-house developed *Matlab* (version 7, http://mathworks.com) scripts and saved in Nifti format. To ease its use with the different software, the voxel size was multiplied by a factor of 10, corresponding to a voxel size of $1.5 \times 1.5 \times 3$ mm^3.

Statistics, clustering and data analysis

Analysis of endocrine and behaviour data was done using IBM SPSS Statistics (v22, http://www.ibm.com/analytics/us/en/technology/spss/spss.html). The normality assumption of all data was verified and subjects with values diverging more than 3 s.d. from the group average were excluded. One control animal from set 1 and three stressed animals (two from set 1 and one from set 2) were excluded. All the data were normalized by transformation into *z*-scores. To classify the animals according to their response to stress after exposure to the 21 days of CUS protocol, a *k*-means clustering algorithm was used inputting the corticosterone levels and the anxiety behaviour marker (time spent in the open arms of the EPM). This algorithm iteratively groups the animals, by creating *k* initial centroids and assigning each animal to the closest centroid and then iteratively re-calculating the centroids from the mean of its assigned animals and re-assigning the animals to each centroid until there are no more changes between iterations. Two cluster centres were used. This allowed us to further divide the stressed animals into high responders (expected high levels of corticosterone and low time spent in the open arms) and low responders (expected low levels of corticosterone and high time spent in the open arms). Comparison between different stress responders and control animals was done using independent samples *t*-test.

For the MRI data, the final groups were made of 21 (13+8, for set one and set two, respectively) controls and 40 CUS. The CUS were further divided into 10 high responders and 10 low responders for set one, and 6 high responders and 14 low responders for set two. For structural MRI data a voxel-based morphometry analysis was conducted. Voxels minimum significance was set as $P < 0.005$ and $P < 0.05$ at the cluster level, corrected for the family-wise error (FWE). For resting-state functional MRI data, a network-based statistics approach was employed using a connection threshold of $P < 0.005$ and $P < 0.05$ at the network level through the network-based statistics approach that corrects for the false discovery rate. We will focus on the result description and discussion on the key hubs of these networks. Hubs are here defined as nodes in the network to which a larger number of significantly affected edges connect when compared with other affected nodes. Without these hubs the affected network would not exist and so they are key in mediating the effects under evaluation. For further details regarding the pre-processing and analysis of MRI data please check the Supplementary Information.

RESULTS

The impact of stress on the neuromatrix

Comparing controls with animals exposed to 21 days of a CUS protocol, we confirmed that, as compared with controls, stressed animals displayed increased plasma levels of corticosterone ($t = 5.126$, d.f. = 39, $P < 0.0001$ and $h = 8.36$ 95% confidence interval (CI) = (6.44–10.29), Figure 1a) and anxious-like behaviour as they displayed reduced open-arm exploration in the EPM ($t = 2.21$, d.f. = 39, $P = 0.033$ and $h = 2.96$ 95% CI = (1.99–4.00), Figure 1b), as assessed in the 2 days preceding the scanning procedures. These results illustrate the overall bioefficacy of the stress protocol used in this study.

Using a voxel-based morphometry approach, we found that 21 days of stress exposure led to a decreased volume of the prelimbic, cingulate, insular, retrosplenial, somatosensory, motor, auditory and perirhinal/entorhinal cortices, the dorsomedial striatum, nucleus accumbens, the septum, the bed nucleus of stria terminalis, the thalamus (anteromedial, anteroventral, mediodorsal, paraventricular posterior), the hippocampus, the mediothalamic tract and mammillary peduncle, the PAG, the interpeduncular, ventral cochlear, trigeminal and facial nuclei (Figures 1c and e; see Supplementary Table 1a for full list of significant FWE-corrected clusters). In addition, we found the overall volume growth of the brain in these subjects (see Supplementary Table 1) to be significantly lower in animals exposed to 21 days of stress.

The analysis of the functional connectome after 21 days of exposure to stress revealed a network that displays increased functional connectivity in the stressed animals (d.f. = 31, $P = 0.029$, $h = 1.27 \pm 0.20$ 95% CI = (1.20–1.35), 13 connections; Figures 1d

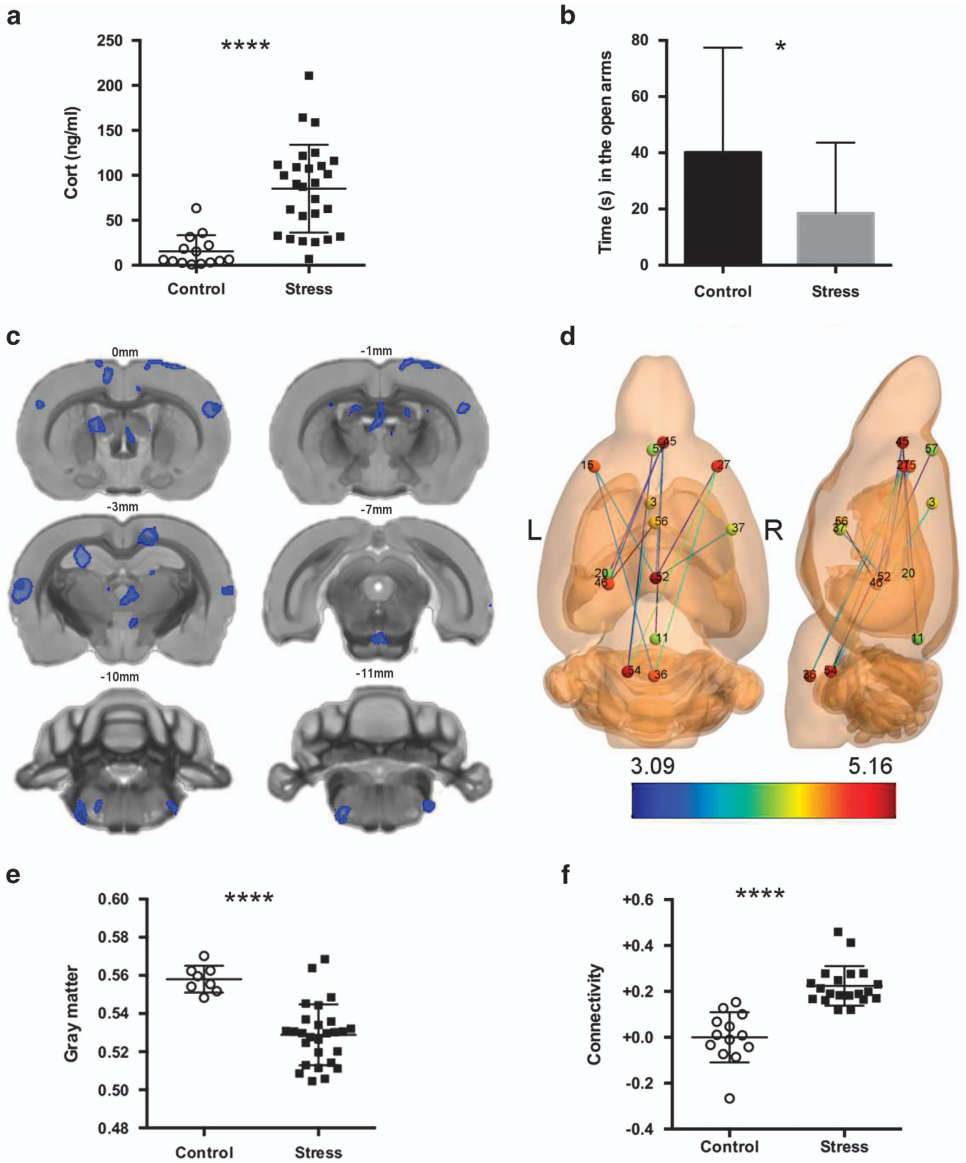

Figure 1. Control versus stressed animal comparison after chronic exposure to stress: (**a**) corticosterone levels as measured at day 21 of stress (significant difference where **** denotes $P < 0.0001$); (**b**) time spent on the open arms of the elevated plus maze (significant difference where * denotes $P = 0.033$); (**c**) clusters of decreased grey matter volume in the stressed animals obtained through voxel-based morphometry (VBM) in blue (voxel-level threshold *P*-uncorrected < 0.005, cluster size > 300 voxels); (**d**) network of increased functional connectivity in the stressed animals as calculated in network-based statistics (NBS; connection-level threshold *P*-uncorrected < 0.005, networks were significant at $P < 0.05$, family-wise error (few) corrected), nodes and edges colour coded according to statistical strength (*t*-value); (**e**) mean modulated grey matter values within the affected areas, where **** denotes $P < 0.0001$, (**f**) mean connectivity within the significant network, where **** denotes $P < 0.0001$.

and 1f; all statistics available in Supplementary Table 3). Two of the internal sub-networks involve brain stem nodes: one links a node involving pontine regions that include the reticular and locus coeruleus/nucleus subcoeruleus (node no. 54) with the cingulate (nos. 3 and 57) and the left primary somatosensory cortices (no. 27), and the other involving the link between the raphe (no. 36) with bilateral primary somatosensory cortices (nos. 15 and 27). The increased connectivity between the thalamus (no. 46) and the hypothalamus (no. 56) is also worth noting, as well as with the prelimbic region of the medial prefrontal cortex (no. 45); the latter has also increased connectivity with the hippocampus (no. 20) and with the retrosplenial cortex (no. 11). Finally, there was an increased connectivity between habenular (no. 52) and amygdalar (no. 37) nodes.

Patterns of stress responses in high and low responders

Next, and given that the response to stress is heterogeneous among distinct individuals (Figures 1a and b), we further categorized the animals' response in two contrasting patterns: high and low responders. For this purpose we used a composite of behavioural (time spent in the open arms) and endocrine (concentration of corticosterone in plasma) data to cluster the animals. The use of this composite allows a more complex separation as not all animals with behaviour deficits present a strong hormonal response, and vice versa. This strategy (a *k*-means clustering, see Supplementary Table 4 for further statistics) allowed us to subdivide the stressed animals in 2 subgroups of 21 high responders (higher levels of corticosterone and more anxious-like behaviour in the EPM) and 27 low responders (lower levels of corticosterone and with less anxious-like behaviour),

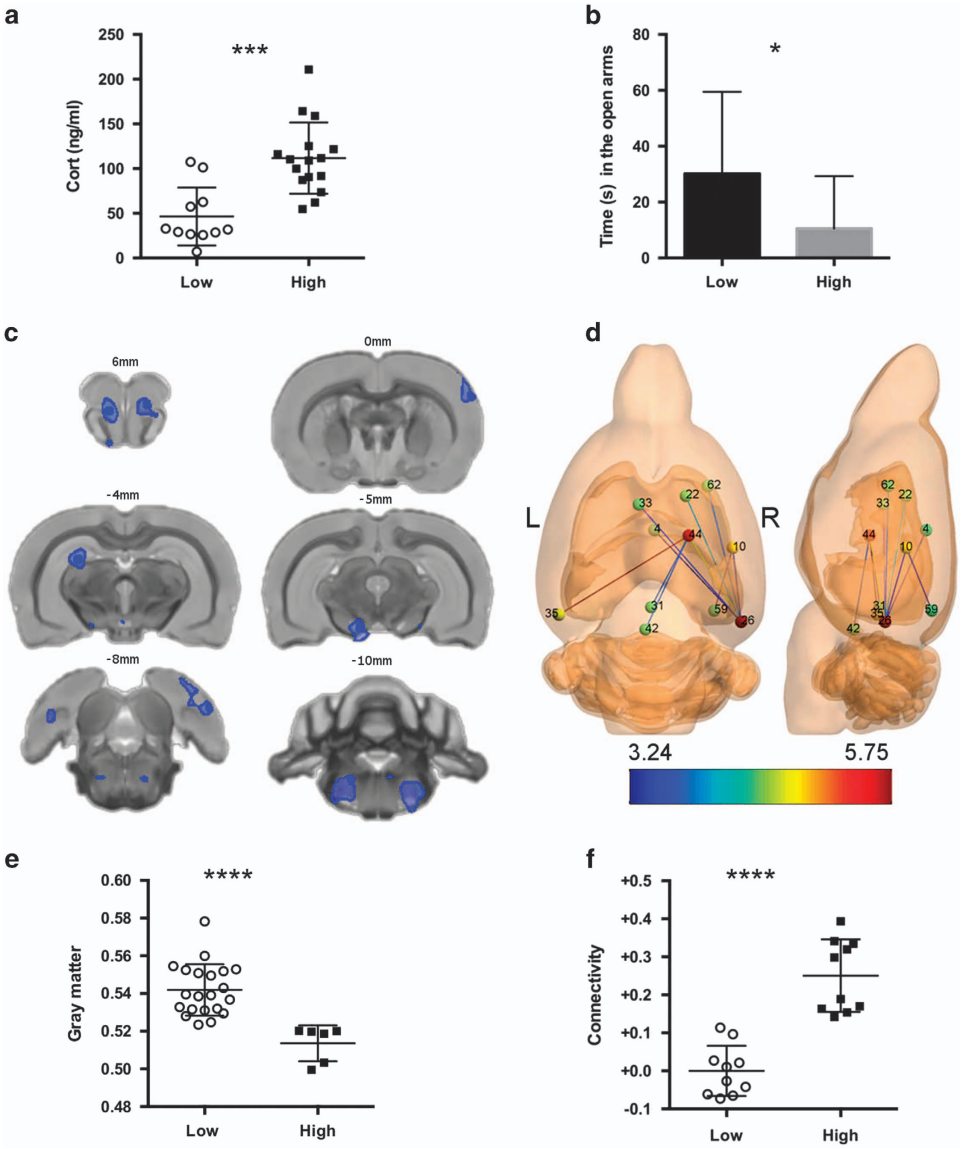

Figure 2. Low- versus high-responder animal comparison after chronic exposure to stress: (**a**) corticosterone levels measured at day 21 of stress (significant difference where *** denotes $P = 0.0001$); (**b**) time spent on the open arms of the elevated plus maze (significant difference where * denotes $P < 0.044$); (**c**) clusters of decreased grey matter volume in the high-responder animals obtained through voxel-based morphometry (VBM) in blue (voxel-level threshold P-uncorrected < 0.005, cluster size > 300 voxels); (**d**) network of increased functional connectivity in the high responders as calculated in network-based statistics (NBS; connection-level threshold P-uncorrected < 0.005, networks were significant at $P < 0.05$ family-wise error (few) corrected), nodes and edges colour coded according to statistical strength (t-value); (**e**) mean modulated grey matter values within the affected areas, where **** denotes $P < 0.0001$; (**f**) mean connectivity within the significant network, where **** denotes $P < 0.0001$.

with significant different levels of corticosterone ($t = 4.50$, d.f. = 25, $P = 0.0001$ and $h = 6.61$ 95% CI = (4.53–8.28), Figure 2a) and time spent in open arms of the EPM ($t = 2.12$, d.f. = 25, $P = 0.044$ and $h = 2.95$ 95% CI = (1.77–3.93), Figure 2b). For a side-by-side comparison of all three final groups please see Supplementary Figure 1.

Restricting the analysis to the subjects who underwent the stress protocol in set one and comparing the brain structure of high and low responders after 21 days of stress, we found a global atrophy in several brain regions, including: ventral orbital cortex, primary somatosensory, retrosplenial and temporal associative cortices, the hippocampal formation, the ventral tegmental area (VTA, paranigral), the hypothalamus (dorsomedial), sensitive trigeminal nucleus and the pontine reticular nucleus regions (parvicellular) (Figures 2c and e; see Supplementary Table 2b for full list of significant FWE-corrected clusters).

When comparing the functional connectome of the high and low responders, we found a network composed of 11 nodes displaying increased functional connectivity in the high responders (d.f. = 18, $P = 0.044$, $h = 1.68$ (1.52–1.82), 10 connections; Figures 2d and e; statistics available in Supplementary Table 2) that can be further subdivided into two main sub-networks. One of these sub-networks has a hub in the right thalamus (no. 44) and is connected with brain stem nodes such as the PAG (no. 31) and ventral tegmental area (no. 42), but also with the subiculum (nos. 26 and 35). Another network has a hub on the subiculum (no. 26) and is linked with the ipsilateral cingulum (no. 4), dorsomedial striatum (nos. 22 and 62) and hippocampus (no. 10). Interestingly, the latter displays increased connectivity with the ipsilateral visual cortex (no. 59). Contrasting with the previous comparison, the affected edges in this network are mostly short-range connections

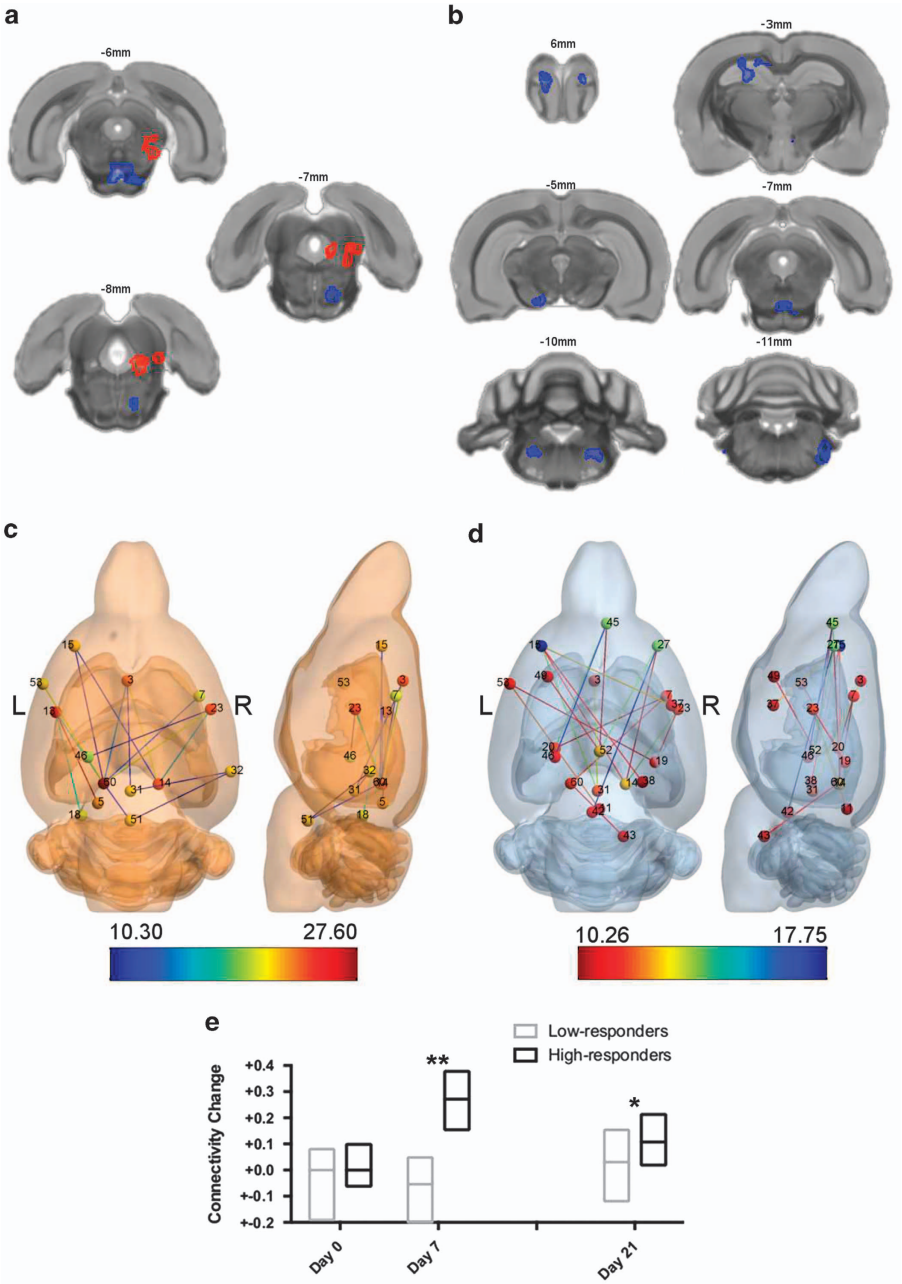

Figure 3. Results from the interaction between response cluster (low and high responders) and stress duration (**a**, **c** between days 0 and day 7; (**b**, **d**) between days 7 and 21). (**a**, **b**) Clusters of grey matter displaying different volume changes obtained through voxel-based morphometry (VBM). Clusters with increasing volumes in high responders compared with low responders are presented in red, and decreasing volumes in blue (voxel-level threshold *P*-uncorrected < 0.005, cluster size > 300 voxels). (**c**, **d**) Network of altered functional connectivity as calculated in network-based statistics (NBS; connection-level threshold *P*-uncorrected < 0.005, networks were significant at $P < 0.05$ family-wise error (few) corrected), nodes and edges colour coded according to statistical strength (F-value). Increasing connectivity in high responders when compared with low responders is coloured in red (days 0 to 7), and decreasing connectivity in blue (days 7 to 21). (**e**) Box plot of mean, minimum and maximum connectivity change within the significant networks of (**c**, **d**) from days 0 to 7 to 21 relative to the day 0 mean. Mean network changes were significant at day 7 (where ** denotes $P < 0.0001$) and day 21 (where * denotes $P < 0.042$).

between posterior (cortical and sub-cortical) and medial thalamic areas (statistics for the comparison of connection length distribution available in Supplementary Table 5 and Supplementary Figure 2).

Temporal dynamics in stress-induced changes

To test the longitudinal temporal dynamics of the stress-induced shifts in brain volumes and in the functional connectome between high and low responders to stress, using the second set of animals, a mixed design analysis of variance was performed with time as repeated measures within-subject factor (days 0, 7 and 21), and cluster (high and low responders) as between- subject factor.

Between days 0 and 7, at the structural level, we found a trend for decreased volumes in the raphe nuclei (paramedian), but increased volumes in the precuneiform and cuneiform nuclei, and in the isthmic reticular formation (Figure 3a; full list of significant FWE-corrected clusters is available in Supplementary Table 2c and d).

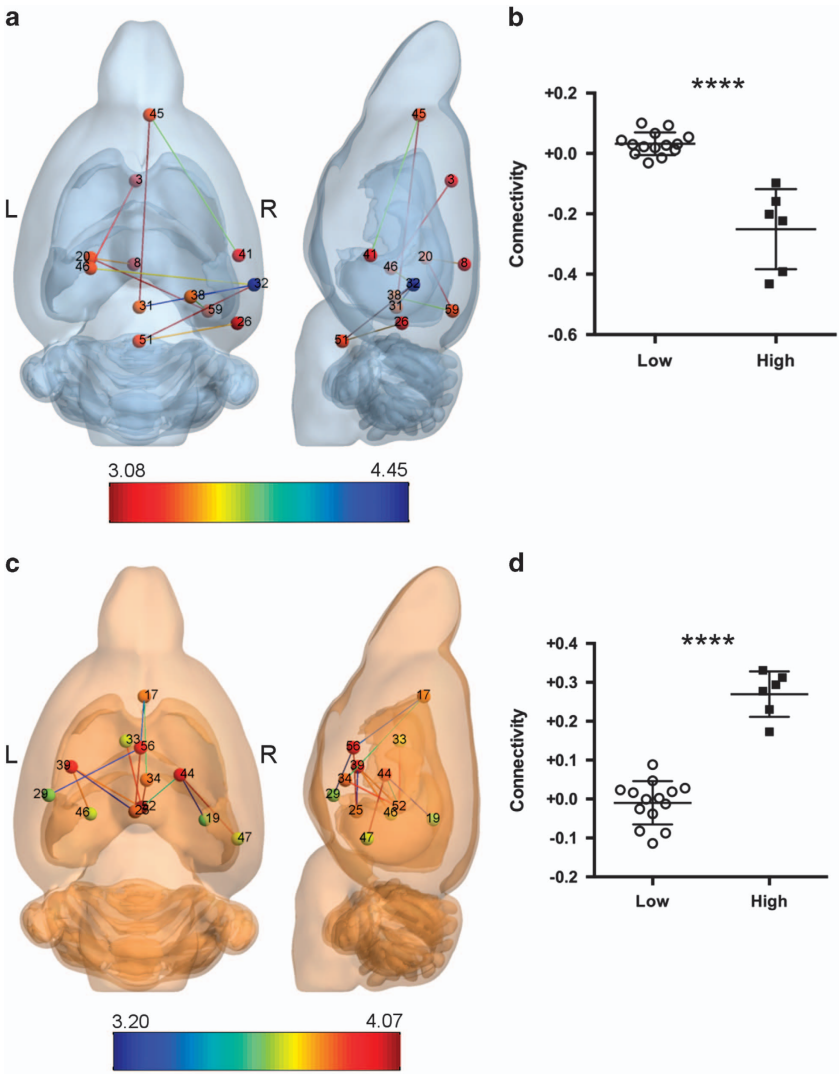

Figure 4. Comparison between animal category (low and high responders) at day 0 (**a**, **b**) and day 7 (**c**, **d**). (**a**, **c**) Network of altered functional connectivity as calculated in network-based statistics (NBS; connection-level threshold *P*-uncorrected < 0.005, networks were significant at $P < 0.05$ family-wise error (FWE) corrected), nodes and edges colour coded according to statistical strength (*t*-value). Decreasing connectivity in high responders when compared with low responders is coloured in blue (day 0), and increasing connectivity in red (day 7). (**b**, **d**) Mean connectivity within the network between animal categories (where **** denotes $P < 0.0001$ in both).

In terms of functional connectivity, we found a network where high-responders showed increasing connectivity, whereas low-responders displayed a very small decrease (d.f. = 1,18, $P = 0.010$, $\eta^2 = 0.20 \pm 0.04$ (0.18–0.21), 16 connections; Figure 3c; all statistics available in Supplementary Table 3). In this network, there were 14 nodes that presented significantly affected edges, with important hubs in the retrosplenial (nos. 14 and 60), somatosensory cortices (nos. 7, 13 and 15) dorsolateral striatum (no. 23) and hippocampus (no. 32). Of notice is the increased connectivity between PAG (no. 31) and cingulate (no. 3), and between the hippocampus (no. 32) and raphe regions (no. 51).

In contrast, between days 7 and 21, there was a widespread reduction in the volumes of the ventral orbital cortex, hippocampus, lateral posterior hypothalamus, substantia nigra (reticular), nucleus interpeduncular and VTA, sensitive trigeminal nucleus and the pontine reticular nucleus regions (parvicellular) (Figure 3b; all significant FWE-corrected clusters are available in Supplementary Table 2e). As for the functional connectome analysis, a significant network was found with decreasing connectivity in high responders that matched with a small increase of connectivity in low responders (d.f. = 1,18, $P = 0.004$, $\eta^2 = 0.19 \pm 0.05$ (0.18–0.21), 19 connections; Figure 3d; all statistics available in Supplementary Table 3). Most significant changes occur in cortical nodes of primary somatosensory cortices (nos. 15 and 27) and their connections to retrosplenial regions (nos. 14 and 60) and to VTA (no. 42) and thalamic regions (no. 52); there is also a strong involvement of prelimbic region of the medial prefrontal cortex (no. 45), thalamic (no. 46), habenular (no. 52), hippocampal (nos. 19 and 20) and PAG (no. 31) nodes. Also of note is the decreased connectivity between hippocampal regions (nos. 19 and 20) and sensory and insular cortices (nos. 23 and 53), as well as between the pontine reticular/subcoeruleus region (no. 43) and the retrosplenial cortex (no. 60). Again, we have an involvement of the frontal cortical areas with long-range connections to posterior areas, although in this case thalamic and hippocampal regions also display a role as can be seen through the presence of more of these nodes and its increased centrality. In Figure 3e we plot the mean network changes from day 0 to day 7 to day 21 revealing that despite the two opposing directions of results, this effect is much stronger in the first week and revealing a mean functional connectivity increase in high responders at day 21 relative to day 0.

Performing the same comparisons with control animals in place of the low responder yielded very similar results (see Supplementary Figure 3 and Supplementary Tables 6 and 7 for all clusters and statistics).

Predictive markers of the response to stress

To test whether the maladaptive response to stress is purely developed during the stress exposure, or whether there are some predictive markers that allow the early identification of vulnerable individuals, independent sample *t*-tests were done at days 0 and 7 between high and low responders.

At day 0 we found a network surviving a connection threshold of $P < 0.0075$, where the high responders have lower connectivity than the low responders; this network is composed by 15 nodes (d.f. = 18, $P = 0.042$, $h = 1.66 \pm 0.22$ (1.57–1.76), 9 connections; Figures 4a and b; see Supplementary Table 3 for all statistics) and includes midbrain PAG (no. 31), median raphe regions (no. 51) and thalamic and hippocampal regions (nos. 20, 38 and 46).

In contrast, at day 7, there was a network of increased connectivity in the high responders (d.f. = 18, $P = 0.027$, $h = 1.48 \pm 0.78$ (1.17–1.80), 12 connections; Figures 4c and d; see Supplementary Table 3 for all statistics) that involves connections between hypothalamic (nos. 34 and 56), thalamic (nos. 44 and 46) and habenular (no. 52) nodes, but also between these regions and the cingulate/prelimbic cortex (no. 17), the amygdala and piriform cortex (nos. 29, 39 and47), the hippocampus (no. 19) and the septum (no. 33). Interestingly, this network mostly involves areas that are known to be critical for the stress response. No significant volumetric variations between high and low responders at day 0 were found.

DISCUSSION

The current work, using voxel-based morphometry, reveals that several brain regions become atrophic after prolonged stress exposure, including numerous cortical areas, the hippocampus and the bed nucleus of stria terminalis. Voxel-based morphometry analysis involve a voxel-wise comparison of the local grey matter concentration. The exact nature and association of these mesoscopic grey matter modifications with neurological and psychiatric dysfunction are still a matter of debate but, generally, variation of grey matter concentration is interpreted as cell size modification, neural or glial cell genesis/apoptosis, spine density or blood flow modifications.[16,17] Our findings are in line with previous studies assessing the morphological impact of stress in the rat brain.[28,33–35] Previous histopathological studies show that a chronic exposure to stress reduces dendritic arborization and synapse density in many of these brain regions, as well as neurogenesis within the hippocampus.[22,36,37]

The next step of our analysis provided another insightful, and biologically more relevant, view of the impact of stress upon the central nervous system. Discriminating between resistant (low responders) and vulnerable (high responders) subjects to a biological challenge is of the utmost importance, but most studies fail to undertake such contrast. The strategy of dividing stressed animals into two groups that display a high versus a low response to stress, based on a composite with behavioural-endocrine measurement, allowed to distinguish the networks, and the nodes, that are critical for such differential response.

This subsequent analysis revealed that some of the stress-induced changes (for example, in the hippocampus) were similarly present in high and low responders, but other changes such as those in the orbital cortex, the VTA, the hypothalamus and the pontine reticular nucleus were specific to high or low responders, suggesting that these areas might be critical for determining a differential response to stress. Interestingly, a previous study described the VTA as a critical node for such maladaptive response to stress, where increased phasic firing of dopaminergic neurons in the VTA was found to be a key factor in determining susceptibility to depression under a social defeat protocol,[38] suggesting a role in passive resilience to stress.[2] Although no structural alterations were previously reported in this context, our results corroborate the important role of this structure. Importantly, alterations in gene expression in the VTA and nucleus accumbens suggest the existence of secondary mechanisms of resilience in these areas that may explain why antidepressants promote adaptations.[39,40]

From the dynamics perspective, the longitudinal analysis of voxel-based morphometry data revealed two different progression patterns marked by small opposite volumetric variations in brain stem nuclei after the first week of stress exposure, with trends for a decrease in the raphe and for an increase in precuneiform and cuneiform nuclei, and in the isthmic reticular formation. Such pattern is followed in subsequent weeks by a reduction in the volumes found in the previous comparison with the addition of the substantia nigra (also a key area of the dopaminergic system), the nucleus interpeduncular and sensitive trigeminal nucleus. These shifts reveal the dynamics of the stress response in terms of structural alterations, and reveal a progression pattern that is mechanistically relevant to understand the causal effects of stress exposure in the whole brain.

Our second dimension of analysis was based on resting-state functional connectomics. This innovative approach allowed us to reveal a network of increased connectivity after stress that includes connections between brain stem and cortical regions, as well as widespread thalamic connections (with the hippocampus, amygdala, prelimbic, insular and retrosplenial cortices), highlighting the role of thalamic regions as a hub in the shifts of connectivity after stress exposure. The increased connectivity might seem a paradoxical result, given that stress exposure is typically viewed as leading to decreased complexity of neuronal connections. Nonetheless, this decrease may result in a reduced specificity and segregation of the networks, and in an overall increase of the synchrony of the signals, a tendency observed in other studies where stress was also found to increase functional connectivity.[25,26]

Comparing different responders to stress, our analysis revealed a hub in the right thalamus, exhibiting an increased connectivity to brain stem nodes such as the PAG and ventral tegmental nucleus, but also with the subiculum and entorhinal cortex. Dendritic remodeling of parts of the thalamus have previously been associated with increased anxious-like behaviour in stressed animals[41] but, to the best of our knowledge, this is the first to report on the key role of this area in mediating the response to stress. In turn, the right subiculum and entorhinal cortex display stronger links with the ipsilateral cingulum, caudate and hippocampus. Connections between the entorhinal cortex and the hippocampus have been shown to play a key role in neurogenesis in the dentate gyrus[42] under the modulatory regulation of glucocorticoids, and anti-depressants are known to improve neurogenesis in the hippocampus by reducing the synchronicity between these regions,[43] an idea supported by our results.

The study of the longitudinal dynamics in the functional connectome between high and low responders to stress exposure also revealed two contrasting events. In the acute phase (days 0to 7) of the stress response, high responders display an increased connectivity in a sub-network that recapitulates well the described acute stress response networks.[44] In contrast, later in the stress exposure (days 7 to 21), even though there is a decreased connectivity in a similar sub-network in high responders, this does not reach the levels of low responders, revealing that the shift to maladaptation to stress results from a faster and more intense initial activation of these networks. Also of note across the functional results is the presence of areas responsible for stimuli

processing, from somatosensory to the visual cortex. Although these areas are not commonly studied in stress, our results seem to indicate that the way that these animals perceive the stressors may be altered through an exacerbation of these circuits.

Comparing the temporal dynamics of the functional and structural alterations, our results seem to point to an interdependence of effects. Considering the changes found during the first week, it seems that the initial changes predominantly occur at the functional level, with increased connectivity within a functional network constituted by several regions commonly related to stress. Such a functional response eventually triggers complementary anatomical alterations in key regions, such as the orbitofrontal cortex and raphe nucleus, that are important in the regulation of the serotonergic system, thus further consolidating the functional alterations at day 21.

Finally, in a retrospective analysis, we decided to search for predictors of differential response to stress. We found, before the start of stress exposure, a functional network where high responders had lower connectivity than low responders, that includes links between mesencephalic reticular regions, pontine raphe regions and thalamic and hippocampal regions. In contrast, later at day 7 of the exposure to stress, we also found that high responders displayed higher connectivity mostly in limbic connections that are known to be critical targets of the stress response, with a focus on the connectivity of the hypothalamus and thalamus with the infralimbic/prelimbic cortices, the amygdala and piriform cortex, the hippocampus and the septum. These findings, especially at day 0, are also consistent with previously published results describing the predictable relationship between anxiety and exploratory behaviour with the development of stress vulnerability.[12–14]

It is important to consider that all the functional data presented here were obtained under anaesthesia. Although we controlled for the effects of variations, isoflurane is known to act as an overall inhibitor of neuronal activity and synchronicity, as measured by functional MRI. These may reduce the effects observed, as more subtle changes may be found if these experiments were conducted in awake rats or during tasks.

In conclusion, the present study reveals a profound impact of stress in the brain that results from two waves of changes, with an inflection point around 1 week after the beginning of the stress exposure (see Supplementary Video where we display first the overall alterations resulting from the comparison of controls and stressed animals, followed by all the differences in the temporal evolution of the low and high responders from days 0 to 21). This inflection point could play an important role in how stress-associated psychiatric conditions are treated, for example, by allowing tailoring of treatments to specific points in the course of psychopathological development. More importantly, we were able to distinguish the neuromatrix of subjects displaying distinct responses to stress and highlight the critical role of the VTA, thalamus and entorhinal cortex in the establishment of a maladaptative response to stress, an interesting avenue to investigate for future pharmacological intervention and therapeutic innovation in psychiatry. Finally, we identified several signatures, namely reduction in connectivity between mesencephalic reticular, pontine raphe, thalamic and hippocampal regions, which may work as potential a priori markers of vulnerability to the harmful effects of stress, serving as likely translatable aids for early diagnosis of stress related brain pathologies.

CONFLICT OF INTEREST

The authors declare no conflict of interest.

ACKNOWLEDGMENTS

This work is part of the Sigma project with the reference FCT-ANR/NEU-OSD/0258/2012 co-financed by the French public funding agency ANR (Agence National pour la Recherche, APP Blanc International II 2012), the Portuguese FCT (Fundação para a Ciência e Tecnologia) and by the Portuguese North Regional Operational Program (ON.2 – O Novo Norte) under the National Strategic Reference Framework (QREN), through the European Regional Development Fund (FEDER) as well as the Projecto Estratégico co-funded by FCT (PEst-C/SAU/LA0026-/2013) and the European Regional Development Fund COMPETE (FCOMP-01-0124-FEDER-037298). DAB and AN were funded by grants from FCT-ANR/NEU-OSD/0258/2012. RM is supported by the FCT fellowship grant with the reference PDE/BDE/113604/2015 from the PhD-iHES program; AC was supported by a grant from the foundation NRJ. PM was funded by Fundação Calouste Gulbenkian (Portugal; 'Better mental health during ageing based on temporal prediction of individual brain ageing trajectories (TEMPO)'), Grant Number P-139977. We thank Drs Patrício Costa and Pedro Moreira for support on the various statistical analyses.

REFERENCES

1 deKloet ER, Joels M, Holsboer F. Stress and the brain: from adaptation to disease. *Nat Rev Neurosci* 2005; **6**: 463–475.
2 Russo SJ, Murrough JW, Han MH, Charney DS, Nestler EJ. Neurobiology of resilience. *Nat Neurosci* 2012; **15**: 1475–1484.
3 Southwick SM, Charney DS. The science of resilience: implications for the prevention and treatment of depression. *Science* 2012; **338**: 79–82.
4 Fleshner M, Maier SF, Lyons DM, Raskind MA. The neurobiology of the stress-resistant brain. *Stress* 2011; **14**: 498–502.
5 Brewin CR, Andrews B, Valentine JD. Meta-analysis of risk factors for posttraumatic stress disorder in trauma-exposed adults. *J Consul Clin Psychol* 2000; **68**: 748–766.
6 Hammen C. Stress and depression. *Annu Rev Clin Psychol* 2005; **1**: 293–319.
7 Melchior M, Caspi A, Milne BJ, Danese A, Poulton R, Moffitt TE. Work stress precipitates depression and anxiety in young, working women and men. *Psychol Med* 2007; **37**: 1119–1129.
8 Welberg L. Psychiatric disorders: a REDD line from stress to depression. *Nat Rev Neurosci* 2014; **15**: 350–351.
9 Fride E, Dan Y, Feldon J, Halevy G, Weinstock M. Effects of prenatal stress on vulnerability to stress in prepubertal and adult rats. *Physiol Behav* 1986; **37**: 681–687.
10 Hougaard KS, Andersen MB, Kjaer SL, Hansen AM, Werge T, Lund SP. Prenatal stress may increase vulnerability to life events: comparison with the effects of prenatal dexamethasone. *Brain Res Dev Brain Res* 2005; **159**: 55–63.
11 Rodrigues AJ, Leao P, Carvalho M, Almeida OF, Sousa N. Potential programming of dopaminergic circuits by early life stress. *Psychopharmacology (Berl)* 2011; **214**: 107–120.
12 Castro JE, Diessler S, Varea E, Marquez C, Larsen MH, Cordero MI *et al.* Personality traits in rats predict vulnerability and resilience to developing stress-induced depression-like behaviors, HPA axis hyper-reactivity and brain changes in pERK1/2 activity. *Psychoneuroendocrinology* 2012; **37**: 1209–1223.
13 Duclot F, Kabbaj M. Individual differences in novelty seeking predict subsequent vulnerability to social defeat through a differential epigenetic regulation of brain-derived neurotrophic factor expression. *J Neurosci* 2013; **33**: 11048–11060.
14 Sandi C, Cordero MI, Ugolini A, Varea E, Caberlotto L, Large CH. Chronic stress-induced alterations in amygdala responsiveness and behavior--modulation by trait anxiety and corticotropin-releasing factor systems. *Eur J Neurosci* 2008; **28**: 1836–1848.
15 Dudley KJ, Li X, Kobor MS, Kippin TE, Bredy TW. Epigenetic mechanisms mediating vulnerability and resilience to psychiatric disorders. *Neurosci Biobehav Rev* 2011; **35**: 1544–1551.
16 Arentsen T, Qian Y, Gkotzis S, Femenia T, Wang T, Udekwu K *et al.* The bacterial peptidoglycan-sensing molecule Pglyrp2 modulates brain development and behavior. *Mol Psychiatry* 2017; **22**: 257–266.
17 Kelly JR, Clarke G, Cryan JF, Dinan TG. Brain-gut-microbiota axis: challenges for translation in psychiatry. *Ann Epidemiol* 2016; **26**: 366–372.
18 Kelly JR, Kennedy PJ, Cryan JF, Dinan TG, Clarke G, Hyland NP. Breaking down the barriers: the gut microbiome, intestinal permeability and stress-related psychiatric disorders. *Front Cell Neurosci* 2015; **9**: 392.
19 Yuen EY, Wei J, Liu W, Zhong P, Li X, Yan Z. Repeated stress causes cognitive impairment by suppressing glutamate receptor expression and function in prefrontal cortex. *Neuron* 2012; **73**: 962–977.
20 Gray JD, Rubin TG, Kogan JF, Marrocco J, Weidmann J, Lindkvist S *et al.* Translational profiling of stress-induced neuroplasticity in the CA3 pyramidal neurons of BDNF Val66Met mice. *Mol Psychiatry* 2016; e-pub ahead of print 13 December 2016; 10.1038/mp.2016.219.

21 Popoli M, Yan Z, McEwen BS, Sanacora G. The stressed synapse: the impact of stress and glucocorticoids on glutamate transmission. *Nat Rev Neurosci* 2011; **13**: 22–37.
22 Sousa N, Lukoyanov NV, Madeira MD, Almeida OF, Paula-Barbosa MM. Reorganization of the morphology of hippocampal neurites and synapses after stress-induced damage correlates with behavioral improvement. *Neuroscience* 2000; **97**: 253–266.
23 Cerqueira JJ, Mailliet F, Almeida OF, Jay TM, Sousa N. The prefrontal cortex as a key target of the maladaptive response to stress. *J Neurosci* 2007; **27**: 2781–2787.
24 Dias-Ferreira E, Sousa JC, Melo I, Morgado P, Mesquita AR, Cerqueira JJ *et al.* Chronic stress causes frontostriatal reorganization and affects decision-making. *Science* 2009; **325**: 621–625.
25 Soares J, Sampaio A, Ferreira LM, Santos NC, Marques P, Marques F *et al.* Stress Impact on Resting State Brain Networks. *PLoS ONE* 2013; **8**: 6.
26 Henckens MJ, van der Marel K, van der Toorn A, Pillai AG, Fernandez G, Dijkhuizen RM *et al.* Stress-induced alterations in large-scale functional networks of the rodent brain. *Neuroimage* 2015; **105**: 312–322.
27 Franklin TB, Saab BJ, Mansuy IM. Neural mechanisms of stress resilience and vulnerability. *Neuron* 2012; **75**: 747–761.
28 Anacker C, Scholz J, O'Donnell KJ, Allemang-Grand R, Diorio J, Bagot RC *et al.* Neuroanatomic differences associated with stress susceptibility and resilience. *Biol Psychiatry* 2016; **79**: 840–849.
29 Magalhaes R, Bourgin J, Boumezbeur F, Marques P, Bottlaender M, Poupon C *et al.* White matter changes in microstructure associated with a maladaptive response to stress in rats. *Transl Psychiatry* 2017; **7**: e1009.
30 Savitz JB, Rauch SL, Drevets WC. Clinical application of brain imaging for the diagnosis of mood disorders: the current state of play. *Mol Psychiatry* 2013; **18**: 528–539.
31 Loeser JD, Melzack R. Pain: an overview. *Lancet* 1999; **353**: 1607–1609.
32 Sousa N. The dynamics of the stress neuromatrix. *Mol Psychiatry* 2016; **21**: 302–312.
33 Bourgin J, Cachia A, Boumezbeur F, Djemaï B, Bottlaender M, Duchesnay E *et al.* Hyper-responsivity to stress in rats is associated with a large increase in amygdala volume. A 7T MRI study. *Eur Neuropsychopharmacol* 2015; **25**: 828–835.
34 Cerqueira JJ, Pêgo J, Taipa R, Bessa JM, Almeida OFX, Sousa N. Morphological correlates of corticosteroid-induced changes in prefrontal cortex-dependent behaviors. *J Neurosci* 2005; **25**: 7792–7800.
35 Soares JM, Sampaio A, Ferreira LM, Santos NC, Marques F, Palha JA *et al.* Stress-induced changes in human decision-making are reversible. *Transl Psychiatry* 2012; **2**: e131.
36 McEwen BS. Stress and hippocampal plasticity. *Annu Rev Neurosci* 1999; **22**: 105–122.
37 Sauro MD, Jorgensen RS, Pedlow CT. Stress, glucocorticoids, and memory: a meta-analytic review. *Stress* 2003; **6**: 235–245.
38 Chaudhury D, Walsh JJ, Friedman AK, Juarez B, Ku SM, Koo JW *et al.* Rapid regulation of depression-related behaviours by control of midbrain dopamine neurons. *Nature* 2013; **493**: 532–536.
39 Krishnan V, Han MH, Graham DL, Berton O, Renthal W, Russo SJ *et al.* Molecular adaptations underlying susceptibility and resistance to social defeat in brain reward regions. *Cell* 2007; **131**: 391–404.
40 Wilkinson MB, Xiao G, Kumar A, LaPlant Q, Renthal W, Sikder D *et al.* Imipramine treatment and resiliency exhibit similar chromatin regulation in the mouse nucleus accumbens in depression models. *J Neurosci* 2009; **29**: 7820–7832.
41 Pego JM, Morgado P, Pinto LG, Cerqueira JJ, Almeida OF, Sousa N. Dissociation of the morphological correlates of stress-induced anxiety and fear. *Eur J Neurosci* 2008; **27**: 1503–1516.
42 Cameron HA, McEwen BS, Gould E. Regulation of adult neurogenesis by excitatory input and NMDA receptor activation in the dentate gyrus. *J Neurosci* 1995; **15**: 4687–4692.
43 Sahay A, Hen R. Adult hippocampal neurogenesis in depression. *Nat Neurosci* 2007; **10**: 1110–1115.
44 Ulrich-Lai YM, Herman JP. Neural regulation of endocrine and autonomic stress responses. *Nat Rev Neurosci* 2009; **10**: 397–409.

Supplementary Information accompanies the paper on the Molecular Psychiatry website (http://www.nature.com/mp)